Microchemical Journal 202 (2024) 110802

Contents lists available at ScienceDirect

Microchemical Journal

journal homepage: www.elsevier.com/locate/microc

An EPR study of the marbles from quarries of the Denizli region (Turkey): A contribution to the provenance assessment of materials with close relationships

Silvia Vettori [a,*], Emma Cantisani [a], Tommaso Ismaelli [a], Giuseppe Scardozzi [b], Antonella Buccianti [c], Francesco Di Benedetto [a,d]

[a] Institute of Heritage Science, National Research Council of Italy (ISPC-CNR), via Madonna del Piano 10, Sesto Fiorentino, 50019 Florence, Italy
[b] Institute of Heritage Science, National Research Council of Italy (ISPC-CNR), via Monteroni, 73100 Lecce, Italy
[c] Department of Earth Sciences, University of Florence, Via G. La Pira, 4, Florence, Italy
[d] Department of Physics and Earth Science, University of Ferrara, via Saragat 1, 44122 Ferrara, Italy

ARTICLE INFO

Keywords:
Quarry provenance
White marbles
Denizli region (Turkey)
EPR spectroscopy
Multivariate statistical data analysis

ABSTRACT

The analytical and spectroscopic discrimination of marbles coming from quarries used in historical times is a task object of a wide interest in archaeometric investigations. This task is even more difficult, when the goal of the provenance assessment is focused on marbles coming from historical quarries located in a close geographic area. In this paper, we present the results of a systematic Electron Paramagnetic Resonance spectroscopy study aimed at assessing the discrimination criteria among 5 quarries located in the Denizli region (Anatolia, Turkey) that were benefited in Hellenistic and Roman period to provide materials for the buildings in the nearby city of Hierapolis of Phrygia (Turkey). The resulting EPR characterisation is used, in combination with the results of isotope geochemistry and petrological observation, to define criteria able to discriminate the provenance of marble samples from the considered quarries. The criteria arose from the analysis operated through robust compositional statistical techniques over the results of the experimental investigation. In this approach, the internal structure of the multimethodic dataset was unravelled. The results here presented provide evidence of a good discriminating ability of the proposed approach.

1. Introduction

The identification of quarry provenance of white marbles is a challenge crossing different disciplines: archaeology, history of art, chemistry, geosciences, conservation science. A consensus claims the impossibility of provenancing a marble by using a single analytical technique. Conversely, numerous approaches, formulating combinations of multiple techniques, have been proposed in the literature [1–11]. Among these approaches, the highly promising method proposed in the early 2000s by Attanasio and coworkers [12–14] involves minero-petrographic analyses, the determination of C and O stable isotopic ratios and the analysis of Electron Paramagnetic Resonance (EPR) spectra of marble samples. Discrimination among provenance groups in the database was usually accomplished through multivariate statistical data analysis, which enables the assignment, with a good probability, of the quarry from which a marble artefact was obtained.

Previous applications of the proposed approach resulted efficient in discriminating the provenance of ancient marbles coming from different regions of the Mediterranean Basin, such as Italian, Greek and Turkish marbles [15–17]. Questions arise if such a method is also able to discriminate the provenance when closer quarries (i.e. linked by close geographical or even geological proximity) are considered. This issue is even more relevant, when the discovery of new ancient quarries or extraction areas force the available database to be updated.

In the present study, we consider the case of the ancient marble quarries in the region of Hierapolis and in the southern sector of the Denizli basin in Turkey. These quarries include both extraction areas previously unknown and never sampled, such as the Marmar Tepe and Gölemezli quarries, and others already known but not systematically investigated, such as the Hierapolis-Gök Dere, Thiounta and Denizli quarries. 47 marble specimens sampled at the five different historical quarries were thus the object of a multi-methodical investigation, which

* Corresponding author.
E-mail address: silvia.vettori@cnr.it (S. Vettori).

https://doi.org/10.1016/j.microc.2024.110802
Received 15 April 2024; Received in revised form 14 May 2024; Accepted 15 May 2024
Available online 17 May 2024

included EPR spectroscopy, minero-petrographic analyses, and determination of C and O stable isotopic ratios, to unravel if their provenance could be assessed by the information experimentally achieved.

2. Previous studies on the marbles from the Denizli region

The Denizli basin, ancient Lykos valley, is an important extractive district in western Anatolia, where the peculiar geological characteristics of the area allowed for the presence of a large variety of building stones and numerous ancient quarries. The research activities carried out between the years 2013–2018 during a previous research project [18] and aimed to reconstruct the building stone procurement strategies adopted in the city of Hierapolis in Phrygia from the Hellenistic age to the Byzantine period. The project also included the archaeometric characterisation both of ancient quarries and marbles used in the building sites of the urban area and necropolises. The research was particularly focused on the white, white veined and grey marbles, which constitute the precious stones most used in Hierapolis and whose provenance is more difficult to define. The systematic study and archaeometric characterization of the white and grey marble quarries of the Denizli basin (and the nearby Uzunpınar plateau), in integration with previous studies [14,19,20,7], constitutes a fundamental basis of knowledge for the provenance determination of the marbles used in the building sites of Hierapolis (and also of the nearby ancient cities in the Lykos valley, such as Laodikeia and Tripolis) [21–23].

The most important result of the archaeological and geological investigations in the Denizli Basin was the identification of five main quarrying areas (Fig. 1) [24], in which different types of marble (white, white-veined and grey) were extracted.

Geologically, the most important features of western Turkey are the grabens that roughly spread from east to west, the basins that turn eastwards from the north, and the horsts that are inserted in between. The Denizli Basin is thus a graben filled with Neogene and Quaternary sediments and bounded on both edges by normal faults. In addition, the graben is divided by a normal fault and extensional fissures. The horsts consist mainly of various types of gneiss, schist and marble from the Menderes Massif and allochthonous Mesozoic carbonates. As for marble, in particular it outcrops (generally in stratigraphic sequence under schist) along the northern and southern edges of the Denizli Basin, overlying the Pamukkale and Babadağ fault zones, respectively (Fig. 1) [25,26].

With regard to the northern slope, marble is found: 1) in the area immediately to the north and north-east of Hierapolis, where it was widely mined in antiquity (Hierapolis-Gök Dere and Marmar Tepe quarries), and 2) to the north of the village of Gölemezli (about 13 km north-west of the Hierapolis city), where other ancient caves can be found [19,21,24]. The Hierapolis-Gök Dere and Marmar Tepe marbles were quarried a short distance from each other. Indeed, the Hierapolis-Gök Dere marble was quarried about 1.5 km north of the city, along the valley of the seasonal stream named Gök Dere, whereas Marmar Tepe marble quarries were identified on the nearby homonymous mountain, about 2 km north of the city. Along the southern slope of the basin, marble outcrops to the south-western outskirts of the modern city of Denizli, in the ancient territory of Laodikeia, where it was also quarried in ancient times [19,21,24]. Here, at least two varieties of marble were identified (named Denizli-1 and Denizli-2). The marble then outcrops north of the basin along the northern end of the Uzunpınar plateau, about 20 km north of Hierapolis, on the two slopes of the upper course of the Menderes river, where mining still continues and the remains of the ancient quarries of Thiounta at Gözler can be found, which are

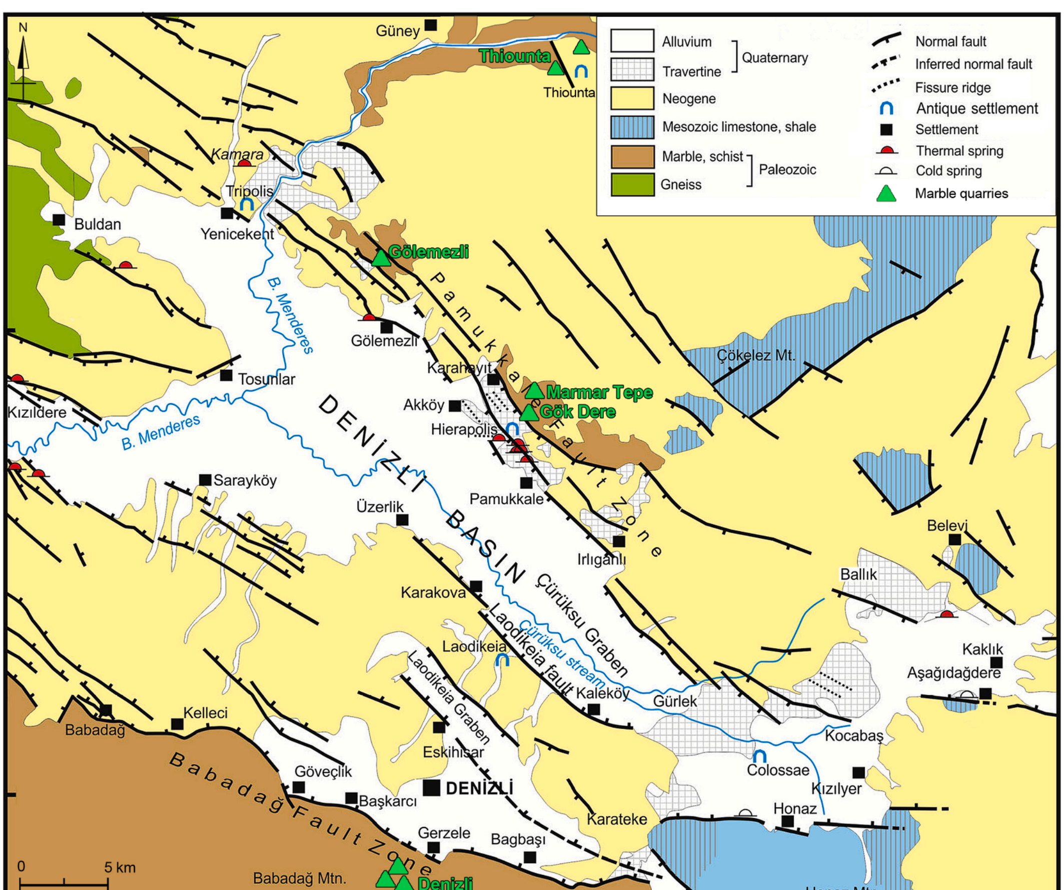

Fig. 1. Simplified geological map of the Denizli basin, with location of the ancient marble quarries. Modified after [24,26].

mentioned in the epigraphic documentation of Hierapolis [21].

The archaeometric characterization of the quarry faces in these extraction areas, thanks to the collection and analyses (minero-petrographic data, C and O isotopic signatures, and cathodoluminescence data) of several samples and the integration of these data with those already available in the literature [19,20,7], allowed for the partial discrimination of these marbles among them and from the other white marbles extracted in south-western Anatolia in antiquity [21,22].

The possibility to discriminate marbles from extraction areas very close to each other is very important to reconstruct the building stone procurement strategies adopted in ancient city of Hierapolis over the centuries [23]. The archaeometric studies of these marbles allowed for the identification of the specific characteristics of the Hierapolis-Gök Dere variety, which is clearly distinguishable from Marmar Tepe, Thiounta, Gölemezli and Denizli-1 marbles due to the C-O isotopic composition (very negative δ^{18}O values). Moreover, it is differentiated from Denizli-2 marble due to its appearance in cathodoluminescence (variable from low to high intensity, and homogeneous/heterogeneous texture). Instead, Marmar Tepe is a very broad and heterogeneous extraction area. The field of isotopic values of Marmar Tepe partly overlaps with that of Gölemezli, which however is distinguished for very high MGS values. Furthermore, in some cases, Marmar Tepe marble shows minero-petrographic texture (such as triple junctions, lineated structures, etc.), C-O isotopic signatures and cathodoluminescence (such as low/medium/high intensity and heterogeneous texture) characteristics allowing it to be distinguished from Thiounta. However, in other cases, Marmar Tepe marble shows minero-petrographic and cathodoluminescence features as well as MGS and C-O isotope values like those of marbles extracted from Thiounta, which prevent a univocal attribution of the unknown archaeological samples.

In this context, the need to discriminate very narrow mining areas to obtain a reliable historical picture asks for the integration of further techniques, in order to disentangle the superposition between the analytical findings related to the different marbles, and to reduce or eliminate the uncertain attributions to different quarries. To this goal, the definition of an accurate protocol for the statistical processing of the data appears needed as well.

3. Experimental procedures

3.1. Investigated samples

47 specimens were investigated in this study and pertain to the five extraction areas cited above. In detail, Table 1 lists the specimen/quarry association. All specimens consist of fragments of marble sampled during a campaign (August 2013) in the site, under the framework of the Marmora Phrygiae project [18]. All the samples were georeferenced using a GNSS. Sampling sites were chosen on the basis of preliminary historical and archaeological considerations. During sampling, particular care was taken in accessing to unexposed rock aliquots, to prevent the sampling of unwanted weathered materials. The chosen sampling locations showed traces of ancient excavation; the samples were collected as uniformly as possible, both vertically and horizontally in relation to the ancient quarry outcrops. The number of samples from each quarry is approximately proportional to the extension of the respective quarry fronts surveyed

Table 1
List of the investigated specimens and related provenance.

Quarry (in bracket the number of specimens)	**Specimen list**
Denizli-1 and Denizli-2 (9)	Denizli-1: D1_1, D2_1, D2_2, D3_1, D3_2, D3bis_2, D4_1 Denizli-2: D5_1, D5_2
Gök Dere (10)	M1bis_1, M1bis_3, M2_1, M2_2, M2bis_2, M4_1, M5_2, M5_3, M5bis_3, M5bis_4
Gölemezli (6)	GM1_1, GM1_2, GM1_3, GM1_4, GM2_1, GM2_2
Marmar Tepe (15)	MT29_2, MT31_1, MT35_1, MT39_1, MT43_1, MT43_2, MT49_1, MT49_3, MT52_1, MT53_1, MT58_1, MT60_1, MT62_1, MT68_1, MT70_1
Thiounta (7)	TH1_1, TH1_4, TH2_1, TH2_2, TH3_1, TH3_2, TH3_3

3.2. EPR spectroscopy

Aliquots of the 47 marble specimens were analyzed by gently grinding by hand an appropriate amount of material to fine powders. The powders were packed in a Teflon bag, which in turn was inserted in amorphous silica tubes. No further manipulation but grinding was operated on the samples, to avoid any possible alteration. The chosen tubes allow avoiding the presence, in the glassy matrix, of transition metal impurities, which would likely interfere with the EPR spectra of the samples.

The EPR spectral measurements were carried out using a conventional Bruker ER 200D-SRC, operating at ~ 9.5 GHz (X-band). All spectra were registered at room temperature according to the following conditions: 0.8 mT modulation amplitude, 100 kHz modulation frequency. The post-amplification gain setup was optimized, sample by sample, maximizing the signal-to-noise ratio. Frequency was calibrated through the reference signal of the DPPH (*1,1-diphenyl-2-pycrylhydrazyl*) radical, used as an external standard. All spectra were registered in the 300–380 mT magnetic field range, with a field step of 0.039 mT and at a scan speed of 0.4 mT/s.

The EPR spectrum of Mn(II), when present and intense enough, was parameterized according to the procedure suggested in the literature [12,14], and accounting for modifications raised by Romanelli et al. [27]. Three parameters (SPREAD, SPLI, WAV) were obtained by five relevant field positions. The reader is referred to these studies for further details in the definition of the spectral parameters. It is noteworthy to recall that the three chosen parameters represent the minimal basis to account for three independent interactions concurring to the final shaping of the EPR spectrum of Mn(II) in calcite. SPREAD, in particular, is mainly determined by the strength of the hyperfine interaction, SPLI refers to the zero-field splitting interaction, whereas WAV refers to both the linewidth and the distribution of fine interaction [27]. The uncertainties in the derived SPREAD, SPLI, WAV values were obtained by propagating the experimental uncertainties in the field position. We also adopted a double blind check of the parameters determination, obtaining standard deviation values definitely smaller than the experimental uncertainty on the parameters.

4. Experimental results

4.1. EPR spectral features

All investigated samples revealed the occurrence of spectra of Mn(II) only. An exemplar EPR spectrum of one of the investigated samples, exhibiting the signal of Mn(II) in the selected field region, is shown in the Fig. 2. The spectral features, in particular the presence of the forbidden hyperfine structure, as well as the peculiar indentation of the sixth allowed hyperfine line, concur to safely attribute the spectrum to Mn replacing Ca in calcite [28] in its distorted octahedral site (point symmetry $\overline{3}$). No evidence, within the experimental detection limit, of the spectral contribution due to Mn(II) replacing for Mg in the Mg site of dolomite [28] was revealed in the whole set of 47 investigated samples. Accordingly, one can conclude that no dolomite is present in the samples, or, at least, that Mn(II) is preferentially partitioned into the calcite lattice.

In the Table 2, the complete list of the experimental values of the EPR parameters defined in the §3 is shown. For all values determined by the EPR parameterisation, the experimental uncertainty is 0.039 mT. Apparently, all spectra revealed the presence of the Mn(II) signal in an

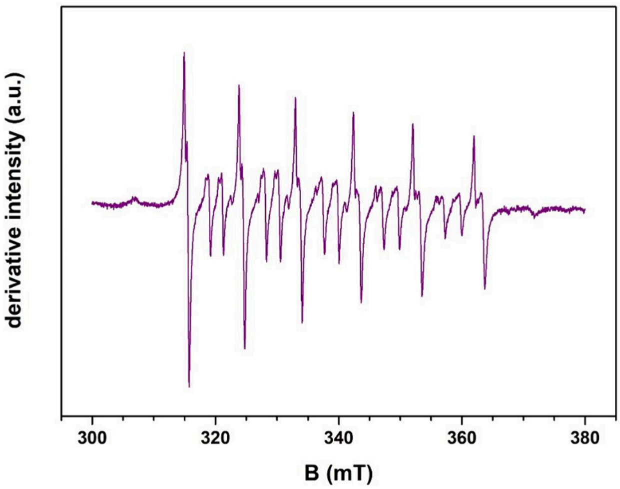

Fig. 2. Exemplar room temperature EPR spectrum of the sample D2.1. Magnetic field values are expressed in mT.

intensity-to-noise ratio suitable for an accurate parameterisation.

5. Discussion

5.1. Internal structure of the EPR dataset

In a first step, the dataset obtained by considering the EPR parameter values only was considered. This db consists of 47 cases and 3 parameters (SPREAD, SPLI and WAV). The three sets of 47 parameter values did not follow a normal distribution due to the presence of skewness and plurimodality (see Supporting information, Section 1), with the exception of SPLI. The closer inspection of the 2 parameters scatter plots, shown in Fig. 2S, (see Supporting information, Section 2), revealed apparent evidence of spurious internal correlation. Accordingly, the information extracted from the EPR spectroscopy cannot be properly described by using the three chosen parameters, but only from a subset of them [29].

This observation was already noticed in a previous study on the statistical analysis of the spectrum of Mn(II) in carbonate rocks [30]. A schematic physical interpretation of the observed internal correlation could link this evidence to the fact that the phenomena traced by the

Table 2
Values of the parameters obtained from the experimental EPR spectra. The parameters SPREAD, SPLI and WAV were obtained by straight parameterisation of the experimental spectra. The irl1 and irl2 parameters were recalculated as defined in the text.

#	label	group	SPREAD (mT)	SPLI (mT)	WAV (mT)	Irl_1	Irl_2
1	D1_1	Denizli	48.764	1.401	0.380	2.516	−2.511
2	D2_1	Denizli	48.785	1.368	0.418	2.423	−2.529
3	D2_2	Denizli	48.777	1.409	0.395	2.485	−2.508
4	D3_1	Denizli	48.777	1.379	0.407	2.458	−2.521
5	D3_2	Denizli	48.775	1.376	0.418	2.426	−2.523
6	D3bis_2	Denizli	48.760	1.441	0.344	2.608	−2.490
7	D4_1	Denizli	48.757	1.381	0.393	2.478	−2.521
8	D5_1	Denizli	48.741	1.425	0.327	2.641	−2.498
9	D5_2	Denizli	48.725	1.431	0.303	2.709	−2.494
10	M1bis_1	Gök Dere	48.814	1.379	0.448	2.378	−2.523
11	M1bis_3	Gök Dere	48.888	1.370	0.567	2.177	−2.527
12	M2_1	Gök Dere	48.814	1.378	0.463	2.342	−2.523
13	M2_2	Gök Dere	48.809	1.389	0.445	2.381	−2.518
14	M2bis_2	Gök Dere	48.785	1.398	0.412	2.452	−2.513
15	M4_1	Gök Dere	48.732	1.377	0.378	2.510	−2.521
16	M5_2	Gök Dere	48.831	1.394	0.498	2.294	−2.514
17	M5_3	Gök Dere	48.840	1.417	0.444	2.388	−2.504
18	M5bis_3	Gök Dere	48.790	1.394	0.415	2.440	−2.515
19	M5bis_4	Gök Dere	48.883	1.353	0.565	2.179	−2.537
20	GM1_1	Gölemezli	48.762	1.404	0.366	2.540	−2.508
21	GM1_2	Gölemezli	48.813	1.361	0.480	2.311	−2.530
22	GM1_3	Gölemezli	48.824	1.393	0.468	2.346	−2.515
23	GM1_4	Gölemezli	48.790	1.361	0.455	2.355	−2.531
24	GM2_1	Gölemezli	48.758	1.415	0.358	2.565	−2.503
25	GM2_2	Gölemezli	48.765	1.404	0.377	2.518	−2.508
26	MT29_2	Marmar Tepe	48.778	1.363	0.418	2.423	−2.529
27	MT31_1	Marmar Tepe	48.705	1.407	0.294	2.730	−2.507
28	MT35_1	Marmar Tepe	48.828	1.351	0.485	2.299	−2.536
29	MT39_1	Marmar Tepe	48.739	1.383	0.409	2.449	−2.518
30	MT43_1	Marmar Tepe	48.716	1.393	0.353	2.571	−2.514
31	MT43_2	Marmar Tepe	48.745	1.378	0.373	2.521	−2.521
32	MT49_1	Marmar Tepe	48.733	1.394	0.349	2.583	−2.514
33	MT49_3	Marmar Tepe	48.714	1.386	0.373	2.524	−2.516
34	MT52_1	Marmar Tepe	48.773	1.401	0.374	2.527	−2.511
35	MT53_1	Marmar Tepe	48.750	1.383	0.373	2.523	−2.519
36	MT58_1	Marmar Tepe	48.720	1.400	0.323	2.648	−2.509
37	MT60_1	Marmar Tepe	48.790	1.370	0.420	2.424	−2.526
38	MT62_1	Marmar Tepe	48.782	1.384	0.408	2.449	−2.518
39	MT68_1	Marmar Tepe	48.776	1.383	0.410	2.447	−2.521
40	MT70_1	Marmar Tepe	48.719	1.386	0.331	2.618	−2.517
41	TH1_1	Thiounta	48.741	1.413	0.361	2.565	−2.503
42	TH1_4	Thiounta	48.859	1.460	0.446	2.401	−2.481
43	TH2_1	Thiounta	48.727	1.414	0.343	2.601	−2.503
44	TH2_2	Thiounta	48.758	1.396	0.400	2.472	−2.513
45	TH3_1	Thiounta	48.732	1.431	0.340	2.617	−2.495
46	TH3_2	Thiounta	48.743	1.348	0.420	2.419	−2.537
47	TH3_3	Thiounta	48.723	1.355	0.449	2.363	−2.534

chosen parameters are not fully discriminated. Following the definition of e.g. SPREAD, three different contributions play a role in the overall separation among the first and the sixth line: 1) the structure due to hyperfine interaction, 2) the two half widths of the first and sixth lines, involved in the WAV definition, and 3) partly, the zero-field splitting of the sixth line, involved in the SPLI definition. Moreover, one could also take into account that line broadening is known to occur with increasing the concentration of the paramagnetic ion (Mn). This could also be relevant on the WAV parameter, but not on the SPLI and SPREAD parameters. The occurrence of the above-cited correlations pointed out the need of unravelling the internal correlation structure of the EPR dataset. This structure was investigated using two different formalisms:

a) by means of the Compositional Data Analysis (CoDA) [29,31], i.e. through the normalisation of the sum of the three parameters, followed by the reduction from a 3D parameter space into a 2D where the dataset expresses its own variability. This was achieved by identifying two isometric coordinates called balances:

$$ilr_1 = \sqrt{\frac{2}{3}} ln \frac{spread}{\sqrt{spli \times wav}} \tag{1}$$

$$ilr_2 = \sqrt{\frac{1}{2}} ln \frac{spli}{wav} \tag{2}$$

The values corresponding to the defined balances are also listed in the Table 2. When plotted in a scatter plot, a very not-spurious good linear correlation has been verified (Supporting information, Section 3);

b) by means of a ternary correlation plot, adopting the procedure to working in the simplex sample space, according to the procedure illustrated and applied in Di Benedetto et al. [32].

One can easily confirm also by this method that a clear linear correlation joins the three variables. In particular, the data in the ternary diagram clearly mark the relative independence of the WAV parameters, whereas the SPLI over SPREAD ratio is almost perfectly constant, irrespective of the change in WAV. One can observe that the two parameters are able to discriminate only partially among the 5 groups (Supporting information, Section 3). Compositional data analysis was performed by using the R package robCompositions [33].

5.2. Analysis of the complete database

The definition of the two new variables in the EPR dataset (i.e. irl1 and irl2) allowed to set up a final database without evidence of internal correlations due to a specific analytical technique. The novel database has the same number of cases, 47, as before, but it is now characterised by 5 relevant variables: irl_1, irl_2, $\delta^{13}C$, $\delta^{18}O$ and MGS. The last three parameters were obtained during the previous research project Marmora Phrygiae and already published in [21,22,24]. The total dimension of the database reaches the 235 values.

In the Fig. 3, the violin plots of the 5 variables discriminated by the sampling provenance are shown. These plots, as well as the following multivariate analysis, have been carried out using the Orange v3.34 code [34]. As apparent, no parameter is able to discriminate among the group provenances, but some variable ranges in the parameter distribution allow to hypothesize a certain degree of discrimination using a multivariate approach.

The complete database identified by the 5 variables and the 47 cases was the object of a multivariate statistical investigation. Preliminary, a dendrogram was realised on the whole database, after having standardised each parameter to its mean and variance, to avoid spurious weights in the comparison of the parameter variability range. The dendrogram was calculated assuming as similarity measure among cases the Euclidean distance and as hierarchical procedure of clustering the Ward linkage method. The result is shown in the Fig. 4a. Apparently, the hierarchy of the branching of the dendrogram allow to identify a group, almost exclusively consisting of the cases of Gök Dere, well isolated from the other cases in the dataset. We decided to support this evidence by a Principal Component Analysis (PCA) approach, still operated on the standardised dataset. Three components result able to trace ∼ 90 % of the dataset variance (Supporting information, Section 4). The component loadings are listed in the Table 3. From the analysis of the loadings, one can conclude that the PC1 component is mainly determined by the irl_1, irl_2 and $\delta^{13}C$ parameters, PC2 by the MGS, $\delta^{13}C$ and $\delta^{18}O$ parameters, and PC3 by MGS and $\delta^{18}O$ parameters. In the Fig. 4b the scatter plot of the scores of the two main PCA components is shown. Apparently, the

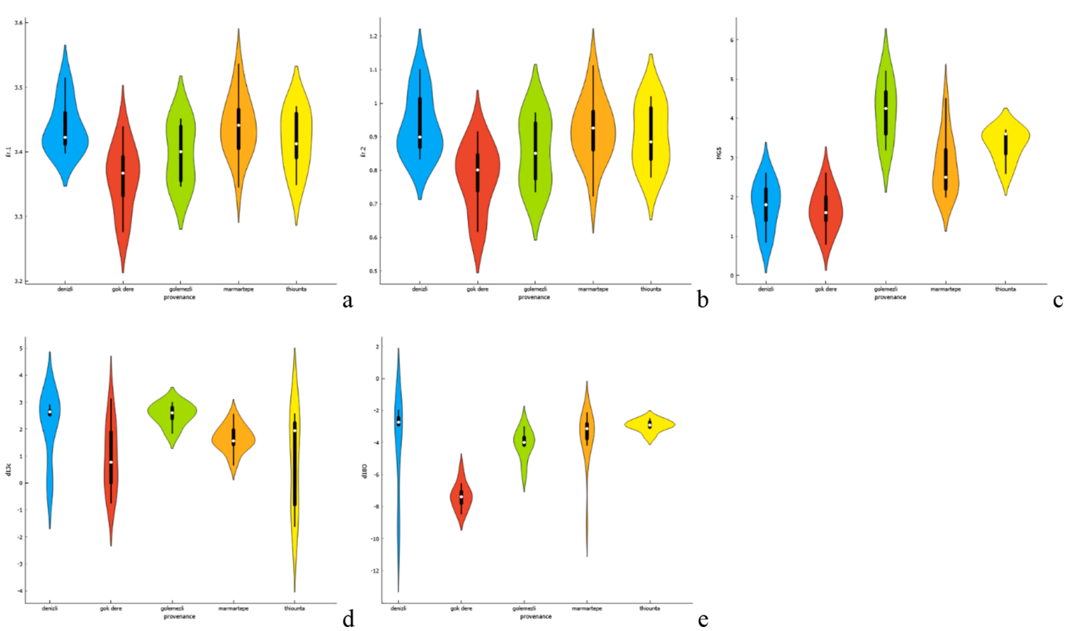

Fig. 3. Violin plots exhibiting the parameter variability for the 5 chosen variables [a) irl1, b) irl2, c) MGS, d) $\delta^{13}C$, e) $\delta^{18}O$], discriminated by provenance [cyan, Denizli; red, Gök Dere; green, Gölemezli; orange, Marmar Tepe; yellow, Thiounta]. (For interpretation of the references to color in this figure legend, the reader is referred to the web version of this article.)

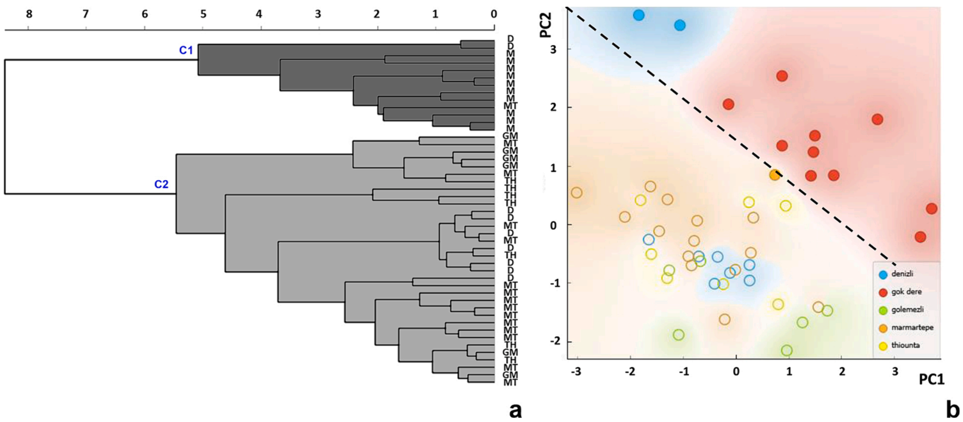

Fig. 4. A) dendrogram of the complete dataset: the groups identified by the first branching are highlighted in grey scale. case provenances are listed at the rights side of the dendrogram (d = Denizli quarry; M = Gök Dere quarry; MT = Marmar Tepe quarry; GM = Gölemezli quarry; TH = Thiounta quarry); b) PC1 versus PC2 scores scatter plot. The cases pertaining to the two groups in the Fig. 4a are marked by full and empty circles, respectively. Color code as in the Fig. 3. A dash line is traced as a guide to the eyes, marking the difference in the graph of the regions where the groups of Fig. 4a plot.

Table 3
Component scores for the PCA analysis of the dataset.

Component	Expl. Variance	Irl1	Irl2	MGS	$\delta^{13}C$	$\delta^{18}O$
PC1	0.40938	−0.679448	−0.674294	−0.033650	−0.273796	−0.087073
PC2	0.32227	0.161995	0.176547	−0.536344	−0.597191	−0.546156
PC3	0.16890	−0.022652	−0.033862	−0.727711	0.011335	0.684579

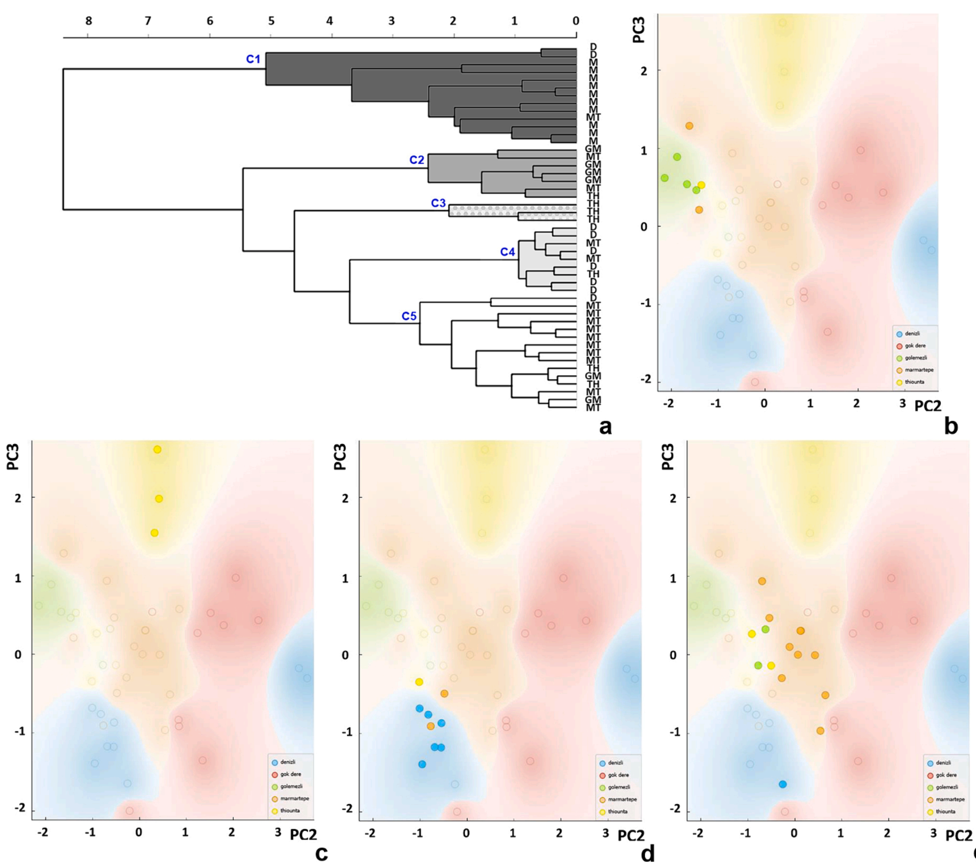

Fig. 5. A) Dendrogram of the complete dataset: the first five groups identified by the main branches are highlighted in grey scale, respectively. provenance labels are listed at the rights side of the dendrogram (d = Denizli quarry; M = Gök Dere quarry; MT = Marmar Tepe quarry; GM = Gölemezli quarry; TH = Thiounta quarry); b-e) PC2 versus PC3 scatter plots, where the cases pertaining to the b) C2, c) C3, d) C4, e) C5 groups in a), are alternatively highlighted as full circles. Colour code as in the Fig. 3.

net discrimination of the cases pertaining to Gök Dere with respect to the others is confirmed and visualized in the variable space. Another interesting point is represented by the appearance in the cluster of two cases, which pertain to the Denizli group. These cases, in fact, are namely the samples D5_1 and D5_2 attributed to a subgroup of the Denizli quarry in the previous study [21]. This evidence has not a statistical significance, of course, because of the limited number of cases.

To go further beyond in the discrimination, we chose to consider the next level (of lower rank) in both the dendrogram and the PCA process. Accordingly, in the light grey group of the dendrogram of Fig. 4a a successive level of branching was considered. One can easily notice that four self-similar groups can be obtained (Fig. 5a). Similarly, in the PCA the loadings and scores of the PCA3 component were also considered. In the Fig. 5b-e, the scatter plot of PC2 versus PC3 is shown. In each graph, only the data pertaining to a single colour are highlighted, to improve the perception of their spatial distribution in the transformed space. Apparently, the plane identified by the 2nd and 3rd components in the transformed space represent a good place where trying to discriminate the four groups identified by the hierarchical cluster analysis. A 3D representation of the multivariate space is also provided in the Supporting information (Section 5). Because of this further analysis, one can observe that the four groups exhibit a clear prevalence of a single provenance, but the discrimination is not complete. Denizli and Marmar Tepe can be evidenced among the four quarries (but Gök Dere) as those best isolated by the statistical analysis of the available database. The "Denizli 1" subgroup, in particular, appears almost well isolated, if one take into account that the subgroup "Denizli-2" subgroup presents a marked affinity with the Gök Dere group.

6. Concluding remarks

The EPR study of the quarries from the Denizli region allowed for the first time to focus this spectroscopic approach in the discrimination of white calcitic marbles coming from sites geographically close and likely geologically correlated. The results obtained in this study clearly show that EPR parameters exhibit a non obvious internal correlation, which limits the numbers of truly independent parameters during the task of provenance assessment. One can attribute this internal correlation in part to a) the parameter definition and b) the Mn concentration. Further studies, aimed at fully characterise the nature and extent of this internal correlation are planned. Nevertheless, at least when operated on pure calcitic marbles (i.e. marbles in which no dolomite content is revealed, or in which Mn is hosted only in the Ca octahedral site in calcite) EPR clearly results to provide additional information for the identification of provenance.

The overall results in the present study are fully in line with those already published on the same samples [21,22], while shedding additional light on the provenance of groups not adequately discriminated by the application of the petrographic and isotopic methods alone. In particular, the net discrimination among the Gök Dere group and the others, already evidenced by Brilli et al. [22], is fully confirmed. Accordingly, we propose the present method as a robust tool to go beyond in the discrimination within datasets emerging from close groups of marbles. The creation of the multimethodic database in which internal correlations have been removed, in particular, allow to sort out internal laws of sample association, which can in turn be used to extend the group discrimination to the highest level achievable given the existing database. With this respect, we can tentatively attribute the non-complete discrimination among the five considered groups of marbles to the limited extent of available samples.

If the discrimination among the group provenance obtained from this study may or may not have a geological and stratigraphic explanation or interpretation is not easy to say. First of all, the metamorphic and tectonic history of the Menderes Massif is extremely complex and not yet fully resolved: if it is the same protolite, if there have been different metamorphic events (Menderes massif, for example, is considered to comprise a sequence of at least four units metamorphosed at variable degree, differently aged and separated mainly by tectonic contacts) [35], if there are different stratigraphic levels. Marble outcrops are, in general, stratigraphically positioned over the schists, especially those in the Hierapolis territory. They also appear in the Paleozoic level of the Massif's upper units and in the Lycian nappes (Mesozoic), which extend past the NE end of the basins, and which house, for example, the Denizli quarries [21]. Unfortunately, we could not find detailed studies about the places where the ancient quarries are. There are only general studies covering very large areas. Further insights in this task will arise from other systematic geological survey.

CRediT authorship contribution statement

Silvia Vettori: Writing – review & editing, Writing – original draft, Visualization, Investigation, Conceptualization. **Emma Cantisani:** Writing – review & editing, Writing – original draft, Visualization, Conceptualization. **Tommaso Ismaelli:** Writing – original draft, Resources, Funding acquisition. **Giuseppe Scardozzi:** Writing – original draft, Resources. **Antonella Buccianti:** Writing – review & editing, Writing – original draft, Methodology, Formal analysis. **Francesco Di Benedetto:** Writing – review & editing, Writing – original draft, Visualization, Supervision, Methodology, Investigation, Funding acquisition, Conceptualization.

Declaration of competing interest

The authors declare the following financial interests/personal relationships which may be considered as potential competing interests: Tommaso Ismaelli reports financial support was provided by National Research Council. Francesco Di Benedetto reports financial support was provided by University of Ferrara. Francesco Di Benedetto reports financial support was provided by University of Ferrara Department of Physics and Earth Sciences. If there are other authors, they declare that they have no known competing financial interests or personal relationships that could have appeared to influence the work reported in this paper.

Data availability

Data will be made available on request.

Acknowledgments

The authors are indebted to Sandra Ristori, for granting the access to the EPR instrumentation at the Dept. of Chemistry of the University of Florence. The authors are also thankful to Prof. Enrico Capezzuoli of the Earth Sciences Department of the University of Florence for his enthusiastic and precious support to the research activity.

The study was supported by the FIRD 2022 and FAR 2023 funds from the Department of Physics and Earth Sciences and from the University of Ferrara, respectively, to Francesco di Benedetto and by CNR FOE 2019 – Technological innovation for protection, enhancement, and safeguard of Cultural Heritage. All funds mentioned are italian.

Appendix A. Supplementary data

Supplementary data to this article can be found online at https://doi.org/10.1016/j.microc.2024.110802.

References

[1] N. Herz, Carbon and oxygen isotopic ratios: a data base for classical Greek and Roman marble, Archaeometry 29 (1) (1987) 35–43, https://doi.org/10.1111/j.1475-4754.1987.tb00395.x.

[2] L. Moens, P. Roos, J. De Rudder, P. De Paepe, J. Van Hende, R. Marechal, M. Waelkens, A multi-method approach to the identification of white marbles used in

antique artifacts, in: N. Herz, M. Waelkens (Eds.) Classical Marble: Geochemistry, Technology, Trade. NATO ASI Series, Springer, Dordrecht, pp. 243–250 https://doi.org/10.1007/978-94-015-7795-3_27.

[3] V. Barbin, K. Ramseyer, D. Decrouez, S.J. Burns, J. Chamay, J.L. Maier, Cathodoluminescence of white marbles: an overview, Archaeometry 34 (2) (1992) 175–183, https://doi.org/10.1111/j.1475-4754.1992.tb00490.x.

[4] C. Gorgoni, L. Lazzarini, P. Pallante, B. Turi, An updated and detailed mineropetrographic and CO stable isotopic reference database for the main Mediterranean marbles used in antiquity, in: J.J. Herrmann, N. Herz, R. Newton (Eds.), ASMOSIA 5: Interdisciplinary Studies on Ancient Stone, Archetype Publications Ltd., London, 2002, pp. 115–131.

[5] S. Capedri, G. Venturelli, A. Photiades, Accessory minerals and $\delta^{18}O$ and $\delta^{13}C$ of marbles from the Mediterranean area, J. Cult. Herit. 5 (1) (2004) 27–47, https://doi.org/10.1016/j.culher.2003.03.003.

[6] M. Brilli, G. Cavazzini, B. Turi, New data of $^{87}Sr/^{86}Sr$ ratio in classical marble: an initial database for marble provenance determination, J. Archaeol. Sci. 32 (10) (2005) 1543–1551, https://doi.org/10.1016/j.jas.2005.04.007.

[7] D. Attanasio, M. Brilli, N. Ogle, The Isotopic Signature of Classical Marbles, Studia Archaeologica, 145, L'Erma di Bretschneider, Roma, 2006.

[8] W. Prochaska, D. Attanasio, in: Interdisciplinary Studies on Ancient Stone, 2012, pp. 230–237.

[9] F. Antonelli, L. Lazzarini, An updated petrographic and isotopic reference database for white marbles used in antiquity, Rend. Lincei 26 (4) (2015) 399–413, https://doi.org/10.1007/s12210-015-0423-4.

[10] G. Poretti, M. Brilli, C. De Vito, A.M. Conte, A. Borghi, D. Günther, A. Zanetti, New considerations on trace elements for quarry provenance investigation of ancient white marbles, J. Cult. Her. 28 (2017) 16–26, https://doi.org/10.1016/j.culher.2017.04.008.

[11] P. Blanc, M.P. Lapuente Mercadal, A. Gutierrez Garcia-Moreno, A new database of the quantitative cathodoluminescence of the main quarry marbles used in antiquity, Minerals 10(4) (2020), 381-397, https://doi.org/10.3390/min10040381.

[12] D. Attanasio, The use of electron spin resonance spectroscopy for determining the provenance of classical marbles, Appl. Magn. Reson. 16 (3) (1999) 383–402, https://doi.org/10.1007/BF03161926.

[13] D. Attanasio, G. Armiento, M. Brilli, M.C. Emanuele, R. Platania, B. Turi, Multimethod marble provenance determinations: the Carrara marbles as a case study for the combined use of isotopic, electron spin resonance and petrographic data, Archaeometry 42 (2) (2000) 257–272, https://doi.org/10.1111/j.1475-4754.2000.tb00881.x.

[14] D. Attanasio, Ancient White Marbles. Identification and analysis by Paramagnetic Resonance Spectroscopy, Studia Archaeologica, L'Erma di Bretschneider, Roma, 2003, p. 122.

[15] D. Attanasio, M. Brilli, M. Bruno, The properties and identification of marble from Proconnesos (Marmara Island, Turkey): a new database including isotopic, EPR and Petrographic Data, Archaeometry 50 (5) (2008) 747–774, https://doi.org/10.1111/j.1475-4754.2007.00364.x.

[16] D. Attanasio, M. Bruno, A.B. Yavuz, Quarries in the region of Aphrodisias: the black and white marbles of Goktepe (Mugla), J. Rom. Archaeol. 22 (2009) 312–348, https://doi.org/10.1017/S1047759400020729.

[17] D. Attanasio, A.B. Yavuz, M. Bruno, J.J. Herrmann Jr, R.H. Tykot, A. Van den Hoek, in: Interdisciplinary Studies on Ancient Stone, 2012, pp. 245–254.

[18] G. Scardozzi, T. Ismaelli, Ancient Quarries and Building Sites in Asia Minor. Research on Hierapolis in Phrygia and Other Cities in South-Western Anatolia: Archaeology, Archaeometry, Conservation, Edipuglia, Bari, Italy, 2016.

[19] T. Koralay, S. Kılınçarslan, Minero-petrographic and isotopic characterization of two antique marble quarries in the Denizli region (western Anatolia, Turkey), Period. Mineral. 84 (2015) 263–288, https://doi.org/10.2451/2015PM0013.

[20] T. Koralay, Archaeometric characterization of the recently discovered Yen sehir marble quarry in the Denizli region, in: T. Ismaelli, G. Scardozzi (Eds.), Ancient Quarries and Building Sites in Asia Minor. Research on Hierapolis in Phrygia and Other Cities in South-Western Anatolia: Archaeology, Archaeometry, Conservation, Edipuglia, Bari, Italy, 2016, pp. 119–130.

[21] M. Brilli, G. Belardi, A.M. Conte, F. Giustini, M.P. Lapuente Mercadal, H. Royo Plumed, G. Quarta, G. Scardozzi, Petrography, geochemistry, and cathodoluminescence of ancient white marble from quarries in the southern Phrygia and northern Caria regions of Turkey: Considerations on provenance discrimination, J. Archaeol. Sci. Rep. 4 (2015) 124–142, https://doi.org/10.1016/j.jasrep.2015.08.036.

[22] [22] M. Brilli, A.M. Conte, F. Giustini, M.P. Lapuente Mercadal, D. Melica, H. Royo Plumed, G. Scardozzi, Archaeometric characterization of white marble from the ancient quarries in the territory of Hierapolis and in the southern sector of the Denizli basin, with an appendix on the Aphrodisian marble, in: T. Ismaelli, G. Scardozzi (Eds.), Ancient Quarries and Building Sites in Asia Minor. Research on Hierapolis in Phrygia and Other Cities in South-Western Anatolia: Archaeology, Archaeometry, Conservation, Edipuglia, Bari, Italy, 2016, pp. 101–118.

[23] [23] G. Quarta, M. Brilli, F. Giustini, M.P. Lapuente Mercadal, D. Melica, T. Ismaelli, H. Royo Plumed, G. Scardozzi, Provenance of the marbles used in the monuments of Hierapolis through an archaeometric approach: Petrography, isotopes and cathodoluminescence, in: T. Ismaelli, G. Scardozzi (Eds.), Ancient Quarries and Building Sites in Asia Minor. Research on Hierapolis in Phrygia and Other Cities in South-Western Anatolia: Archaeology, Archaeometry, Conservation, Edipuglia, Bari, Italy, 2016, pp. 183–230.

[24] G. Scardozzi, The provenance of marbles and alabasters used in the monuments of Hierapolis in Phrygia (Turkey): new information from a systematic review and integration of archaeological and archaeometric data, Heritage 2 (2019) 519–552, https://doi.org/10.3390/heritage2010035.

[25] M. Özkul, S. Kele, A. Gökgöz, C.C. Shen, B. Jones, M.O. Baykara, I. Fòrizs, T. Németh, Y.W. Chang, M.C. Alçiçek, Comparison of the Quaternary travertine sites in the Denizli extensional basin based on their depositional and geochemical data, Sedimen. Geol. 294 (2013) 179–204, https://doi.org/10.1016/j.sedgeo.2013.05.018.

[26] H. Kumsar, O. Aydan, C. Şimsek, F. D'Andria, Historical earthquakes that damaged Hierapolis and Laodikeia antique cities and their implications for earthquake potential of Denizli basin in western Turkey, Bull. Eng. Geol. Environ. 75 (2) (2015) 519–536, https://doi.org/10.1007/s10064-015-0791-0.

[27] M. Romanelli, A. Buccianti, F. Di Benedetto, L. Bellucci, S. Cemicky, An innovative electron paramagnetic resonance and statistical analysis approach to investigate the geographical origin of multi-layered samples from a Renaissance painting, Microchem. J. 177 (2022) 107219–107228, https://doi.org/10.1016/j.microc.2022.107219.

[28] R.A. Shepherd, W.R.M. Graham, EPR of Mn^{2+} in polycrystalline dolomite, J. Chem. Phys. 81 (1984) 6080–6084, https://doi.org/10.1063/1.447612.

[29] J. Aitchison, The statistical analysis of compositional data, Lts., London, Monographs on statistics and applied probability, Chapman and Hall, 1986.

[30] F. Di Benedetto, A. Buccianti, G. Montegrossi, M. Innocenti, C.A. Massa, L.A. Pardi, M. Romanelli, EPR discrimination of microcrystalline calcite geomaterials, Am. Mineral. 97 (10) (2012) 1619–1626, https://doi.org/10.2138/am.2012.4168.

[31] J.J. Egozcue, V. Pawlowsky-Glahn, G. Mateu-Figueras, C. Barcelo-Vidal, Isometric logratio transformations for compositional data analysis, Math. Geol. 35 (3) (2003) 279–300, https://doi.org/10.1023/A:1023818214614.

[32] F. Di Benedetto, A. Giaccherini, G. Montegrossi, L.A. Pardi, A. Zoleo, F. Capolupo, M. Innocenti, G.O. Lepore, F. D'Acapito, F. Capacci, C. Poli, T.E. Iaia, A. Buccianti, M. Romanelli, Chemical variability of artificial stone powders in relation to their health effects, Sci Rep. 9 (1) (2019) 6531–6544, https://doi.org/10.1038/s41598-019-42238-2.

[33] RobComposition package, version 2.4.1 in R: A language and environment for statistical computing. R Foundation for Statistical Computing, Vienna, Austria, (2023), URL https://www.R-project.org/.

[34] J. Demsar, T. Curk, A. Erjavec, C. Gorup, T. Hocevar, M. Milutinovic, M. Mozina, M. Polajnar, M. Toplak, A. Staric, M. Stajdohar, L. Umek, L. Zagar, J. Zbontar, M. Zitnik, B. Zupan, Orange: Data Mining Toolbox in Python, J. Mach. Learn. Res. 14 (2013) 2349–2353.

[35] K. Gessner, U. Ring, C.W. Passchier, C. Johnson, R. Hetzel, T. Gungor, An active bivergent rolling-hinge detachment system: central Menderes metamorphic core complex in western Turkey, Geology 29 (2001) 611–614, https://doi.org/10.1130/0091-7613(2001)029%3C0611:AABRHD%3E2.0.CO;2.